IEEE TRANSACTIONS ON AEROSPACE AND ELECTRONIC SYSTEMS Volume 55, Issue 4, 2019, pp. 1843-1849
DOI: 10.1109/TAES.2018.2876588

Integral Global Sliding Mode Guidance for Impact Angle Control

Shaoming He, Defu Lin and Jiang Wang

***Abstract*—This Correspondence proposes a new guidance law based on integral sliding mode control (ISMC) technique for maneuvering target interception with impact angle constraint. A time-varying function weighted line-of-sight (LOS) error dynamics, representing the nominal guidance performance, is introduced first. The proposed guidance law is derived by utilizing ISMC to follow the desired error dynamics. The convergence of the guidance law developed is supported by Lyapunov stability. Simulations with extensive comparisons explicitly demonstrate the effectiveness of the proposed approach.**

I. Introduction

The final approach angle of an interceptor to a target is known as the impact angle. Constraining this impact angle is often desirable for increasing the warhead effectiveness as well as the kill probability since it enables the missile to attack a vulnerable spot on a target. For this reason, over the past decades, extensive efforts have been done in the area of impact angle control for tactical missiles. The two most well-known categories of impact angle constrained guidance laws are: optimal guidance law [1]–[6] and biased proportional navigation guidance (BPNG) law [7]–[9]. Optimal guidance laws bring in the philosophy of trajectory optimization while developing guidance laws, thereby optimizing a meaningful cost function as well as meeting the terminal boundary conditions. In comparison, BPNG laws use a biased term to control the impact angle while the capturability is guaranteed by the nominal PNG part in an attempt to nullify the LOS rate. Most of these guidance laws are derived by admitting linearized kinematics subject to small angle assumption.

With the development of modern control theory, some elegant solutions were also reported to control the impact angle. Among them, sliding mode control (SMC) has found wide acceptance in guidance law design due to its inherent robustness against matched disturbances [10]–[18]. A guidance law with a dual linear sliding surface was suggested in [12] to cater for impact angle constraint against maneuvering targets. The guidance law switches between two sliding surfaces governed by the capturability condition, which is determined by the sign of the closing velocity. An improved result by terminal SMC (TSMC) was developed in [13], providing the property of finite-time convergence of LOS angle errors. To circumvent the inherent singularity associated with TSMC, nonsingular TSMC (NTSMC) was employed in [14]–[16] to derive impact angle control guidance laws. In a recent noteworthy contribution [17], a switching logic between NTSM sliding surface and general linear sliding surface was exploited in guidance law design. The additional linear sliding surface was employed to obtain the one-to-one mapping from impact angle to LOS angle. This guidance law is applicable for speed-disadvantaged interceptors and thus extends the application of NTSM guidance law.

Apart from regular SMC, the concept of ISMC, proposed in [19], provides engineers an alternative way to design SMC with guaranteed global sliding manifold, i.e. the reaching phase is eliminated. Owing to this benefit, the state response under ISMC is predictable from its nominal part, enabling the flexibility of designing the equivalent controller. This implies that the convergence pattern of the tracking errors can be shaped as desired. This reason leads to the selection of ISMC in this paper. Note that ISMC was adopted in [20] for guidance law design to improve the performance of the well-known PNG law, which was incapable of controlling the impact angle.

Motivated by the above observations, this Correspondence considers designing guidance laws to intercept maneuvering targets by utilizing ISMC methodology for impact angle control. A time-to-go weighted desired LOS error dynamics, which determines the nominal guidance performance, is in introduced first. Theoretical analysis shows that both the LOS angle error and its rate along the desired error dynamics approach zero simultaneously at the time of impact. Based on the LOS error dynamics developed, the ISMC methodology is utilized to design guidance law to force the system trajectory to follow the desired dynamics. The advantage of the proposed guidance law lies in that the guidance performance can be easily predicted by the equivalent control part, guaranteeing the nominal performance imposed by the weighted LOS error dynamics.

The remainder of the Correspondence is organized as follows. The necessary backgrounds and preliminaries are stated in Sec. II. The proposed error dynamics and its property are provided in Sec. III. In Sec. IV, the proposed guidance law is derived in details, followed by the simulation results shown in Sec. V. Finally, some concluding remarks are offered.

This work was supported by the National Natural Science Foundation of China under Grant No. 61172182 and the Fundamental Research Project of Beijing Institute of Technology under Grant No. 20130142017.

Shaoming He is with the School of Aerospace, Transportation and Manufacturing, Cranfield University, Cranfield MK43 0AL, UK (email: shaoming.he.cn@gmail.com)

Defu Lin is with the Institute of UAV Autonomous Control, Beijing Institute of Technology, Beijing 100081, P.R. China (email: lindf@bit.edu.cn)

Jiang Wang (Corresponding Author) is with the School of Aerospace Engineering, Beijing Institute of Technology, Beijing 100081, P.R. China (email: wjbest200@163.com)

II. Backgrounds and Preliminaries

This section first provides some necessary preliminaries about the missile-target relative kinematics model. Then, the problem formulation of this paper is stated.

A. Missile-Target Relative Kinematics

This paper considers a two-dimensional planar homing engagement geometry shown in Fig. 1. As presented in the geometry, the inertial reference frame is denoted as (X, Y). Variables with subscripts of M and T denote those of the missile and target, respectively. The notations of λ and r are the LOS angle and the missile-target relative range. γ denotes the flight path angle defined in the inertial reference frame. The velocity and lateral acceleration are represented by V and a, respectively. For simplicity, it is assumed both the missile and the target are flying with constant velocity.

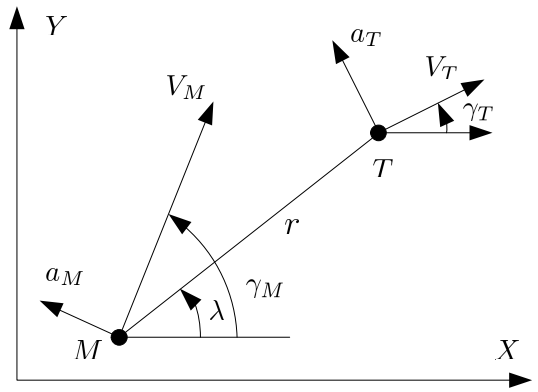

Fig. 1. Planar engagement geometry.

The corresponding equations describing the missile-target relative motion kinematics can be formulated as

$$\dot{r} = V_T \cos(\gamma_T - \lambda) - V_M \cos(\gamma_M - \lambda) \tag{1}$$

$$r\dot{\lambda} = V_T \sin(\gamma_T - \lambda) - V_M \sin(\gamma_M - \lambda) \tag{2}$$

The complementary equations defining the relationship between the flight path angle and lateral acceleration are

$$\dot{\gamma}_M = \frac{a_M}{V_M} \tag{3}$$

$$\dot{\gamma}_T = \frac{a_T}{V_T} \tag{4}$$

Let $V_r \triangleq \dot{r}$, $V_\lambda \triangleq r\dot{\lambda}$ be the relative velocities along and perpendicular to the LOS, respectively. Then, differentiating Eq. (1) and (2) with respect to time yields

$$\dot{V}_r = \frac{V_\lambda^2}{r} + a_{Tr} - a_M \sin(\lambda - \gamma_M) \tag{5}$$

$$\dot{V}_\lambda = -\frac{V_r V_\lambda}{r} + a_{T\lambda} - a_M \cos(\lambda - \gamma_M) \tag{6}$$

where $a_{Tr} \triangleq a_T \sin(\lambda - \gamma_T)$, $a_{T\lambda} \triangleq a_T \cos(\lambda - \gamma_T)$ denote the target acceleration along and normal to the LOS, respectively.

B. Problem Formulation

To ensure target capture, the missile should have to impose hard constraints on terminal miss distance as well as terminal impact angle error. The term impact angle, denoted as θ_{imp}, is defined as the angle between the missile velocity vector and the target velocity vector, i.e. $\theta_{imp} \triangleq \gamma_T - \gamma_M$. Assuming a perfect interception is achieved, i.e. $\dot{\lambda} = 0$, it follows from Eq. (2) that

$$V_T \sin(\gamma_T - \lambda) = V_M \sin(\gamma_M - \lambda) \tag{7}$$

which reveals that, for a pre-designated target with an expected impact angle, there always exists a corresponding desired terminal LOS angle. Let λ_F be the desired LOS angle, solving Eq. (7) for λ_F yields

$$\lambda_F = \gamma_T - \tan^{-1}\left(\frac{\sin\theta_{imp}}{\cos\theta_{imp} - V_T/V_M}\right) \tag{8}$$

Assume $V_T/V_M < 1$, then Eq. (8) provides an one-to-one mapping from the impact angle to the LOS angle. This means that the control of impact angle can be transformed to LOS angle tracking problem. Also notice that zeroing the LOS rate $\dot{\lambda}$ leads to perfect interception with zero miss distance [21]. The objective of this paper is therefore to design a LOS shaping guidance law a_M in such a way that the missile can capture a maneuvering target with desired LOS angle λ_F.

Remark 1. For speed-disadvantaged missiles, the condition of one-to-one mapping from the impact angle to the LOS angle is violated as stated in [17] and one can use the dual sliding mode method suggested in [17] to solve the multiple solution problem.

III. Line-of-Sight Error Dynamics and Analysis

This section introduces the proposed error dynamics, determining the nominal guidance performance, and presents its closed-form solution to analyze the characteristics.

A. Proposed Error Dynamics

To begin with, define $e \triangleq \lambda - \lambda_F$ as the LOS angle tracking error and consider the following generalized second-order time-varying error dynamics

$$\ddot{e} + \frac{a}{t_{go}}\dot{e} + \frac{b}{t_{go}^2}e = 0 \tag{9}$$

where $a > 0$, $b > 0$ are gains that regulate the convergence rate of the error dynamics. The time-to-go t_{go} from Eq. (9) is approximated using range over range rate as

$$t_{go} = -\frac{r}{\dot{r}} \tag{10}$$

By selecting this formulation for the error dynamics (9), the LOS angular error and LOS angular rate error can be shown to converge to zero at the final impact time.

Remark 2. Although approximation (10) tends to be smaller than the real time-to-go during the initial flight period, especially for impact angle control trajectory [2]–[5], this fact only affects the convergence rate of the error dynamics and has no

effect on the final tracking error. Actually, it follows from Eq. (9) that smaller t_{go} results in larger gains, leading to faster convergence rate. The approximated t_{go}, which is calculated in every guidance command update step, converges to the real time-to-go towards the end of the engagement.

B. Characteristics of the Proposed Error Dynamics

To analyze the characteristics of error dynamics (9), we seek to find its closed-form solution. It can be noted that Eq. (9) is a second-order Cauchy-Euler differential equation with respect to t_{go}. In this paper, we restrict to different real number roots of the characteristic equation of Eq. (9). To this end, consider

$$e = ct_{go}^{n} \tag{11}$$

as a special solution of Eq. (9), where c and n are two nonzero constants. Taking the first and second order time derivatives of Eq. (11) gives

$$\dot{e} = -cnt_{go}^{n-1}, \quad \ddot{e} = cn\left(n-1\right)t_{go}^{n-2} \tag{12}$$

Substitution of Eq. (12) in error dynamics (9) and collecting the same powers of t_{go} yields

$$\left[n\left(n-1\right)-an+b\right]t_{go}^{n-2} = 0 \tag{13}$$

Solving Eq. (13) results in two roots as

$$n_1 = \frac{a+1+\sqrt{(a+1)^2-4b}}{2}, \quad n_2 = \frac{a+1-\sqrt{(a+1)^2-4b}}{2} \tag{14}$$

Since this paper only considers different real number roots of the characteristic equation, we have $a+1 > 2\sqrt{b}$. Define the parameterization $a = k_1 + k_2$, $b = (k_1+1)\,k_2$, where k_1, k_2 are two design parameters. Then, Eq. (14) can be reduced to

$$n_1 = k_1 + 1, \quad n_2 = k_2 \tag{15}$$

Since $n_1 > n_2$, one can conclude that $k_1 + 1 > k_2$. Substituting Eq. (15) into Eq. (11) gives the generic solution of Eq. (9) as

$$e = c_1(t_f - t)^{n_1} + c_2(t_f - t)^{n_2} \tag{16}$$

where c_1, c_2 are two constants governed by the initial conditions. Applying the initial boundary conditions on the generic solution (16) generates

$$c_1 = \frac{n_2 e\left(0\right) + t_f \dot{e}\left(0\right)}{n_2 - n_1} t_f^{-n_1}, \quad c_2 = \frac{n_1 e\left(0\right) + t_f \dot{e}\left(0\right)}{n_1 - n_2} t_f^{-n_2} \tag{17}$$

Differentiating Eq. (16) with respect to time yields

$$\dot{e} = -c_1 n_1 (t_f - t)^{n_1 - 1} - c_2 n_2 (t_f - t)^{n_2 - 1} \tag{18}$$

It follows from Eqs. (16) and (18) that both the LOS angle error and LOS rate error converge to zero at the time of impact if $n_1 > 1$, $n_2 > 1$ or the equivalent form $k_1 > 0$, $k_2 > 1$. Since $k_1 + 1 > k_2$, the required condition reduces to $k_2 > 1$. The closed-form solution, shown in Eqs. (16) and (18), reveals that, by choosing different coefficients k_1, k_2, different convergence rates of the LOS angle tracking error can be achieved and therefore the guidance command can be correspondingly shaped in a desired way.

Remark 3. Different from the error dynamics proposed in [11], where the coefficients are tuned using offline optimization, a and b in error dynamics (9) can be easily chosen to achieve desired convergence pattern of the LOS errors by using the closed-form solutions. Also, guidance law proposed in [11] only apply to non-maneuvering targets while the proposed algorithm can be applied to maneuvering targets.

IV. Guidance Law Design and Implementation

In this section, error dynamics (9) is utilized for impact angle control guidance law design to intercept maneuvering targets. It follows from Eq. (8) that $\dot{\lambda}_F = \dot{\gamma}_T = a_T/V_T$, $\ddot{\lambda}_F = \dot{a}_T/V_T$. To force the system trajectory onto the desired error dynamics (9), we propose the following integral sliding surface

$$s = \dot{e} + z = \dot{\lambda} - \frac{a_T}{V_T} + z \tag{19}$$

where

$$z = \int \left(\frac{a}{t_{go}}\dot{e} + \frac{b}{t_{go}^2}e\right)dt, \quad z\big(0\big) = -\dot{e} \tag{20}$$

which guarantees the global sliding manifold, e.g., $s(0) = 0$. It is easy to verify that the LOS angle error dynamics reduces to Eq. (9) when $s(0) = 0$. This means that the guidance performance can be easily predicted by the closed-form solution of the proposed error dynamics.

Differentiating Eq. (19) with respect to time and substituting Eq. (6) into it yields

$$\dot{s} = -\frac{\dot{a}_T}{V_T} - \frac{2\dot{r}\dot{\lambda}}{r} + \frac{a_{Tr}}{r} - \frac{a_M \cos\left(\lambda - \gamma_M\right)}{r} + \frac{a}{t_{go}}\dot{e} + \frac{b}{t_{go}^2}e \tag{21}$$

The proposed guidance law is formulated as

$$\begin{aligned} a_M &= a_M^{eq} + a_M^{add} \\ a_M^{eq} &= \frac{1}{\cos\left(\lambda - \gamma_M\right)}\left(-\frac{r\dot{a}_T}{V_T} - 2\dot{r}\dot{\lambda} + a_{Tr} - \frac{a}{t_{go}}\dot{e}r + \frac{b}{t_{go}^2}er\right) \\ a_M^{add} &= \frac{rM|s|^{\alpha}\mathrm{sgn}\left(\mathrm{s}\right)}{\cos\left(\lambda - \gamma_M\right)} \end{aligned} \tag{22}$$

From Eq. (19), one can note that the sliding surface for maneuvering targets interception with impact angle constraint requires the information on target maneuver. This is a typical requirement for other SMC impact angle guidance laws [12], [13], [16]. In implementation, the target maneuver information can be estimated using some well-established approaches, see second-order sliding mode observer [22], [23] and adaptive observer [24] for examples. The guidance command (22) also reveals that the implementation of the proposed guidance law needs the information on the rate of target maneuver, also known as target jerk. However, accurate estimation for this hidden state is difficult to be extracted from the available measurements. Fortunately, due to the fact that every target is a mechanical system with physical limits, it is reasonable to assume that $\dot{a}_T/V_T$ is a small variable. This assumption is very natural since fast changing of acceleration is quite difficult for mechanical systems because of limited actuator bandwidth, especially for aerodynamically-controlled vehicles.

Therefore, one can safely remove the term $r\dot{a}_T/V_T$ in Eq. (22) with ignorable effect on the guidance performance. With this simple modification, Eq. (22) reduces to

$$a_M = \frac{1}{\cos(\lambda-\gamma_M)}\left[-2\dot{r}\dot{\lambda} + a_{Tr} - \frac{a}{t_{go}}\dot{e}r + \frac{b}{t_{go}^2}er + Mrsig^{\alpha}(s)\right] \tag{23}$$

Moreover, due to the existence of the robust term $M\text{sig}^{\alpha}(s)$, the effect of $r\dot{a}_T/V_T$ on guidance precision can be further reduced to a relatively low level. To see this, consider $V = 0.5s^2$ as a Lyapunov function candidate. Define $\Delta \triangleq -\dot{a}_T/V_T$, taking the time derivative of the Lyapunov function and substituting Eqs. (21) and (23) into it yields

$$\begin{aligned}\dot{V} &= s\left(-\frac{\dot{a}_T}{V_T} - \frac{2\dot{r}\dot{\lambda}}{r} + \frac{a_{Tr}}{r} - \frac{a_M\cos(\lambda-\gamma_M)}{r} + \frac{a}{t_{go}}\dot{e} + \frac{b}{t_{go}^2}e\right)\\ &= s\left(-\frac{\dot{a}_T}{V_T} - Msig^{\alpha}(s)\right)\\ &= s\left(\Delta - Msig^{\alpha}(s)\right)\\ &\le |s|\left(|\Delta| - M|s|^{\alpha}\right)\end{aligned} \tag{24}$$

which reveals that if $|s| \ge (|\Delta|/M)^{1/\alpha}$, $\dot{V} \le 0$. This means that by removing the jerk term in guidance command (22), the sliding variable can still be ensured to be in a small region around zero by $|s| < (|\Delta|/M)^{1/\alpha}$. Since Δ is a small variable and $1/\alpha > 1$, one can imply that the upper bound of the compact region is very close to zero and thus the effect of the jerk term is ignorable.

Remark 4. Note that inequality (24) also provides us the rule for tuning the guidance gain M: choosing M as an increasing function with respect to time. Such kind of guidance gain gradually shrinks the region boundary of the sliding dynamics when the missile approaches the target, thereby leading to accurate interception. For instance, one can set the guidance gain inversely proportional to the relative range as $M(t) = M_0/r$ with M_0 being a positive constant and we utilize this type of guidance gain in our simulation studies.

V. Simulation Results

In this section, the performance of the proposed guidance law is investigated through numerical simulations under various conditions. In all simulations, a point-mass missile model with a lag-free autopilot dynamics is used. The coefficients of the proposed LOS error dynamics are chosen as $a = 6$, $b = 12$. The guidance gain M_0 is set as $M_0 = 50$ and the smoothing parameter α is selected as $\alpha = 0.8$ in all scenario tests without any further tunings. The initial conditions and different scenarios of the engagement considered here are summarized in Tables I and II, respectively.

In order to demonstrate the superiority of the proposed guidance law, the existing NTSM impact angle guidance law [16] is also performed in simulations for the purpose of comparison. The NTSM guidance law is defined as

$$\begin{aligned}&s = (\lambda-\lambda^*) + l\left(\dot{\lambda} - \tfrac{a_T}{V_T}\right)^{\eta}, l>0, \eta = \tfrac{p}{q}, p>q\\ &\text{sgmf}(x) = 2\left(\tfrac{1}{1+\exp^{-\kappa x}} - \tfrac{1}{2}\right), \quad \kappa > 0\\ &a_M = \tfrac{1}{\cos(\lambda-\gamma_M)}\left[-2\dot{r}\dot{\lambda} + \tfrac{r}{\eta l}\left(\dot{\lambda} - \tfrac{a_T}{V_T}\right)^{(2-\eta)}\right] + \tfrac{K}{\text{sgmf}(\cos(\lambda-\gamma_M))}\text{sgmf}(s)\end{aligned} \tag{25}$$

where p, q are two positive odd integers satisfy $1 < \eta < 2$, $K > 0$ the switching gain. The continuous function $\text{sgmf}(x)$ is used to replace the original discontinuous sign function for the purpose of chattering mitigation. In order to make fair comparisons, the design parameters, which are well-tuned to provide good overall performance in [16], are used here in simulations.

Fig. 2 compares the missile trajectory of the proposed guidance law with that of NTSM guidance law for the four considered scenarios. Fig. 3 shows the impact angle profiles produced by the guidance laws. These figures show that both guidance laws successfully intercept the target with desired impact angles. The recorded miss distances of these two guidance laws in these scenarios are less than 0.1795 m and the impact angle errors in these scenarios are less than 0.239 deg. Fig. 2 clearly shows that NTSM guidance law exhibits more curved trajectories in some scenarios, vertical interception for instance. Figs. 4 and 5 show the time history of the LOS angle tracking error and LOS rate tracking error, respectively. It follows from these figures that both LOS angle tracking error and its rate converge to zero at the time of impact under both guidance laws. Therefore, capturability and impact angle control are guaranteed. The missile acceleration command of different guidance laws are displayed in Fig. 6. The control efforts of all guidance laws are summarized in Table III. From this table, we observe that the NTSM guidance law requires more control efforts than the proposed ISMC guidance law in all scenarios, especially in the vertical interception missions. The reason of this phenomenon is clear: the proposed ISMC guidance law removes the reaching phase and thus requires less control effort.

TABLE I
INITIAL CONDITIONS FOR HOMING ENGAGEMENT.

Parameters	Values
Missile-target initial relative range, $r(0)$	$10000m$
Initial LOS angle, $\lambda(0)$	30°
Missile velocity, V_M	$500m/s$
Missile initial flight path angle, $\gamma_M(0)$	45°
Target velocity, V_T	$250m/s$
Target initial flight path angle, $\gamma_T(0)$	108°

TABLE II
DIFFERENT SCENARIOS FOR HOMING ENGAGEMENT.

Scenario	Parameters
Scenario 1	$a_T = -20m/s^2, \theta_{imp} = 180^\circ$
Scenario 2	$a_T = -20m/s^2, \theta_{imp} = 90^\circ$
Scenario 3	$a_T = 20\sin(0.1\pi t)\, m/s^2, \theta_{imp} = 180^\circ$
Scenario 4	$a_T = 20\sin(0.1\pi t)\, m/s^2, \theta_{imp} = 90^\circ$

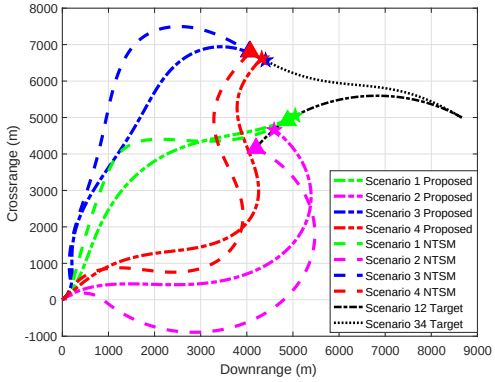

Fig. 2. Interception trajectory.

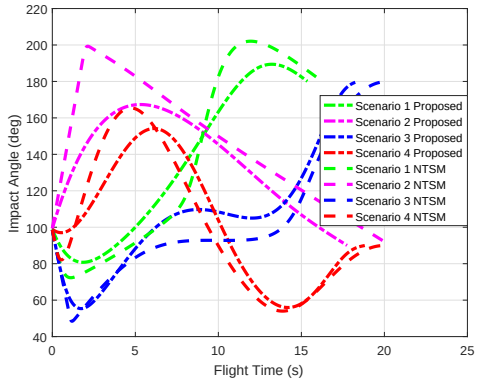

Fig. 3. Impact angle.

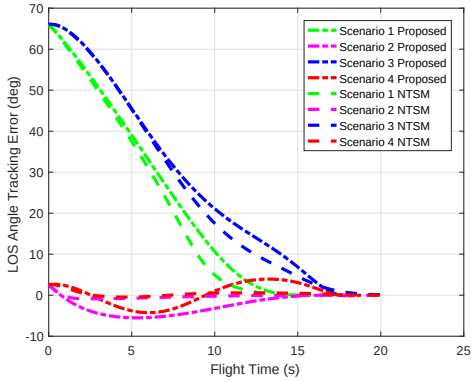

Fig. 4. LOS angle tracking error.

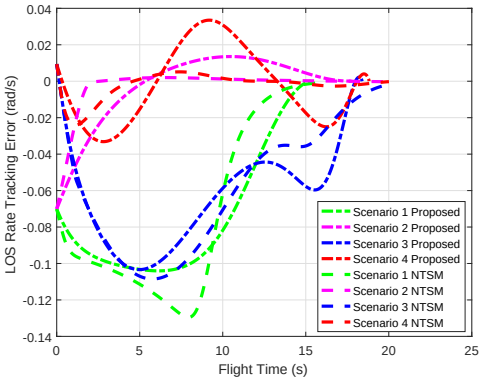

Fig. 5. LOS rate tracking error.

VI. Conclusions

This Correspondence proposes a new approach for impact angle control guidance by following the designed LOS error dynamics using ISMC methodology. The prominent feature of the proposed LOS error dynamics lies in that both the LOS angle tracking error and its rate converge to zero at the time of impact, thus leading to accurate interception. The advantage of the proposed guidance law lies in that it enables flexibility of designing the nominal control part by virtue of the proposed weighted LOS shaping concept. Simulation results with some comparisons clearly confirm the effectiveness of the proposed guidance laws.

References

[1] M. Kim and K. V. Grider, "Terminal guidance for impact attitude angle constrained flight trajectories," *IEEE Transactions on Aerospace and Electronic Systems*, no. 6, pp. 852–859, 1973.

[2] C.-K. Ryoo, H. Cho, and M.-J. Tahk, "Time-to-go weighted optimal guidance with impact angle constraints," *IEEE Transactions on Control Systems Technology*, vol. 14, no. 3, pp. 483–492, 2006.

[3] A. Ratnoo and D. Ghose, "State-dependent riccati-equation-based guidance law for impact-angle-constrained trajectories," *Journal of Guidance, Control, and Dynamics*, vol. 32, no. 1, p. 320, 2009.

[4] Y.-I. Lee, S.-H. Kim, J.-I. Lee, and M.-J. Tahk, "Analytic solutions of generalized impact-angle-control guidance law for first-order lag system," *Journal of Guidance, Control, and Dynamics*, vol. 36, no. 1, pp. 96–112, 2012.

[5] C.-K. Ryoo, H. Cho, and M.-J. Tahk, "Optimal guidance laws with terminal impact angle constraint," *Journal of Guidance Control and Dynamics*, vol. 28, no. 4, pp. 724–732, 2005.

[6] E. J. Ohlmeyer and C. A. Phillips, "Generalized vector explicit guidance," *Journal of Guidance, Control, and Dynamics*, vol. 29, no. 2, pp. 261–268, 2006.

[7] B. S. Kim, J. G. Lee, and H. S. Han, "Biased png law for impact with

TABLE III
CONTROL EFFORTS OF ALL GUIDANCE LAWS.

Guidance law	Scenario 1	Scenario 2	Scenario 3	Scenario 4
Proposed	95839	160972	157667	168310
NTSM	138345	247311	170184	231128

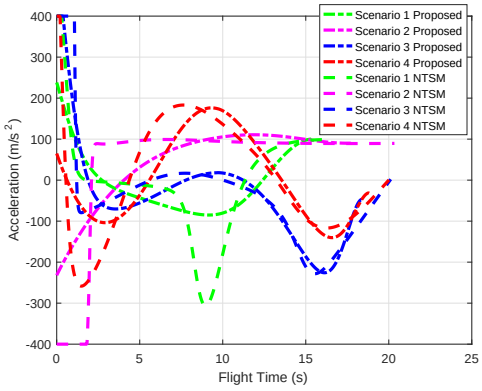

Fig. 6. Acceleration command.

angular constraint," *IEEE Transactions on Aerospace and Electronic Systems*, vol. 34, no. 1, pp. 277–288, 1998.
[8] A. Ratnoo and D. Ghose, "Impact angle constrained interception of stationary targets," *Journal of Guidance, Control, and Dynamics*, vol. 31, no. 6, p. 1817, 2008.
[9] K. S. Erer and O. Merttopçuoglu, "Indirect impact-angle-control against stationary targets using biased pure proportional navigation," *Journal of Guidance, Control, and Dynamics*, vol. 35, no. 2, pp. 700–704, 2012.
[10] S. Rao and D. Ghose, "Sliding mode control-based autopilots for leaderless consensus of unmanned aerial vehicles," *IEEE Transactions on Control Systems Technology*, vol. 22, no. 5, pp. 1964–1972, 2014.
[11] N. Harl and S. Balakrishnan, "Impact time and angle guidance with sliding mode control," *IEEE Transactions on Control Systems Technology*, vol. 20, no. 6, pp. 1436–1449, 2012.
[12] S. Rao and D. Ghose, "Terminal impact angle constrained guidance laws using variable structure systems theory," *IEEE Transactions on Control Systems Technology*, vol. 21, no. 6, pp. 2350–2359, 2013.
[13] S. R. Kumar, S. Rao, and D. Ghose, "Sliding-mode guidance and control for all-aspect interceptors with terminal angle constraints," *Journal of Guidance, Control and Dynamics*, vol. 35, no. 4, pp. 1230–1246, 2012.
[14] ——, "Non-singular terminal sliding mode guidance and control with terminal angle constraints for non-maneuvering targets," in *Variable Structure Systems (VSS), 2012 12th International Workshop on*. IEEE, 2012, pp. 291–296.
[15] S. He, D. Lin, and J. Wang, "Continuous second-order sliding mode based impact angle guidance law," *Aerospace Science and Technology*, vol. 41, pp. 199–208, 2015.
[16] S. R. Kumar, S. Rao, and D. Ghose, "Nonsingular terminal sliding mode guidance with impact angle constraints," *Journal of Guidance, Control, and Dynamics*, vol. 37, no. 4, pp. 1114–1130, 2014.
[17] Z. Hou, L. Liu, Y. Wang, J. Huang, and H. Fan, "Terminal impact angle constraint guidance with dual sliding surfaces and model-free target acceleration estimator," *IEEE Transactions on Control Systems Technology*, vol. 25, no. 1, pp. 85–100, 2017.
[18] S. He, T. Song, and D. Lin, "Impact angle constrained integrated guidance and control for maneuvering target interception," *Journal of Guidance, Control, and Dynamics*, vol. 40, no. 10, pp. 2653–2661, 2017.
[19] V. Utkin and J. Shi, "Integral sliding mode in systems operating under uncertainty conditions," in *Decision and Control, 1996., Proceedings of the 35th IEEE Conference on*, vol. 4. IEEE, 1996, pp. 4591–4596.
[20] Y.-W. Liang, C.-C. Chen, D.-C. Liaw, Y.-C. Feng, C.-C. Cheng, and C.-H. Chen, "Robust guidance law via integral-sliding-mode scheme," *Journal of Guidance, Control, and Dynamics*, vol. 37, no. 3, pp. 1038–1042, 2014.
[21] R. W. Morgan, H. Tharp, and T. L. Vincent, "Minimum energy guidance for aerodynamically controlled missiles," *IEEE Transactions on Automatic Control*, vol. 56, no. 9, pp. 2026–2037, 2011.
[22] Y. B. Shtessel, I. A. Shkolnikov, and A. Levant, "Smooth second-order sliding modes: Missile guidance application," *Automatica*, vol. 43, no. 8, pp. 1470–1476, 2007.
[23] ——, "Guidance and control of missile interceptor using second-order sliding modes," *IEEE Transactions on Aerospace and Electronic Systems*, vol. 45, no. 1, pp. 110–124, 2009.
[24] N. Hovakimyan and C. Cao, $\mathcal{L}_1$ *Adaptive Control Theory: Guaranteed Robustness with Fast Adaptation*. SIAM, 2010.